

University of Nebraska - Lincoln

DigitalCommons@University of Nebraska - Lincoln

US Department of Energy Publications

U.S. Department of Energy

1988

IN-SITU STRESS ORIENTATION AND MAGNITUDE AT THE FENTON GEOTHERMAL SITE, NEW MEXICO, DETERMINED FROM WELLBORE BREAKOUTS

Colleen A. Barton

Stanford University

Mark D. Zoback

Stanford University, zoback@stanford.edu

Kerry L. Burns

Los Alamos National Laboratory

Follow this and additional works at: <https://digitalcommons.unl.edu/usdoepub>



Part of the [Bioresource and Agricultural Engineering Commons](#)

Barton, Colleen A.; Zoback, Mark D.; and Burns, Kerry L., "IN-SITU STRESS ORIENTATION AND MAGNITUDE AT THE FENTON GEOTHERMAL SITE, NEW MEXICO, DETERMINED FROM WELLBORE BREAKOUTS" (1988). *US Department of Energy Publications*. 87.

<https://digitalcommons.unl.edu/usdoepub/87>

This Article is brought to you for free and open access by the U.S. Department of Energy at DigitalCommons@University of Nebraska - Lincoln. It has been accepted for inclusion in US Department of Energy Publications by an authorized administrator of DigitalCommons@University of Nebraska - Lincoln.

IN-SITU STRESS ORIENTATION AND MAGNITUDE AT THE FENTON GEOTHERMAL SITE, NEW MEXICO, DETERMINED FROM WELLBORE BREAKOUTS

Colleen A. Barton and Mark D. Zoback

Department of Geophysics, Stanford University, California

Kerry L. Burns

Los Alamos National Laboratory, New Mexico

Abstract. The acoustic borehole televiewer provides excellent data for the detection and measurement of stress-induced wellbore breakouts. Analog televiewer data from the Fenton Geothermal well EE-3 in New Mexico were digitized and interactively processed for detection and analysis of azimuth and shape of stress-induced breakouts occurring in the well at depths of about 2.9 - 3.5 km. A statistical analysis of the measured breakout azimuths yields a well resolved orientation of least horizontal principal stress of 119° , consistent with least principal stress data from the Rio Grande Rift. As the magnitude of the least horizontal compressive stress, Sh_{min} , in EE-3 is known from hydraulic fracturing, we present a new method in which Sh_{min} and data on breakout width are used to estimate the magnitude of the maximum horizontal principal stress.

Introduction

Stress-induced wellbore breakouts have become important as indicators of the direction of horizontal principal stresses [e.g. Bell and Gough, 1979; Hickman, et al., 1985; Plumb and Cox, 1986]. Their mechanism of formation was first discussed by Gough and Bell [1981] and later expanded upon by Zoback et al., [1985]. Breakouts are the result of localized shear failure around a borehole in response to horizontal compression. This compression creates spalling in symmetric zones around the borehole at the azimuth of least horizontal principal stress where the circumferential compressive stress is greatest. Correlation of breakout data with independent stress measurements has demonstrated that breakouts give reliable stress orientations in the upper crust [Zoback and Zoback, 1988].

Site Location and Stress History

Situated on the western boundary of the Rio Grande rift, data collected at the Fenton Geothermal well provide stress information for a complex, tectonically active region (Figure 1, after Aldrich et al., 1986). The Rio Grande rift is an intraplate rift that trends NNE from south central New Mexico to central Colorado [Chapin and Cather, 1981]. It is bounded by the Great Plains and Southern Rocky Mountains to the east and by the Colorado Plateau and Basin and Range to the west. Rifting in this region began between 25 and 29 m.y. ago. It is geologically active today and is characterized by high heat flow, high seismicity, vertical crustal movements, recent volcanism, shallow magma bodies and a thin lithosphere [Golombek, 1983; Olsen et al., 1986; Cordell, 1978]. The Fenton Geothermal well is drilled 4018 m into the Precambrian basement underlying 1500 meters of 1.1 - 1.4 m.y. tuffs and Mesozoic and Paleozoic sediments of the Jemez Mountains. The well is located within the transition zone between the

Colorado Plateau and the Rio Grande rift [Zoback and Zoback, 1980, 1988]. Within this transition zone, in-situ stress indicators show variation in the direction of ambient horizontal compressive stresses (Figure 1).

Data Acquisition

The borehole televiewer is an ultrasonic well-logging tool useful for measuring the orientation and distribution of fractures and lithostratigraphic features [Zemanek, 1970]. The televiewer contains a rotating acoustic transducer that emits a focused 3° beam pulse at a rate of 1800 times a second. The 1.4 Mhz transducer rotates three revolutions per second and moves vertically up the borehole at a speed of 2.5 cm/s. Ultrasonic seismograms are transmitted through a standard wireline logging cable and recorded on videotape. A

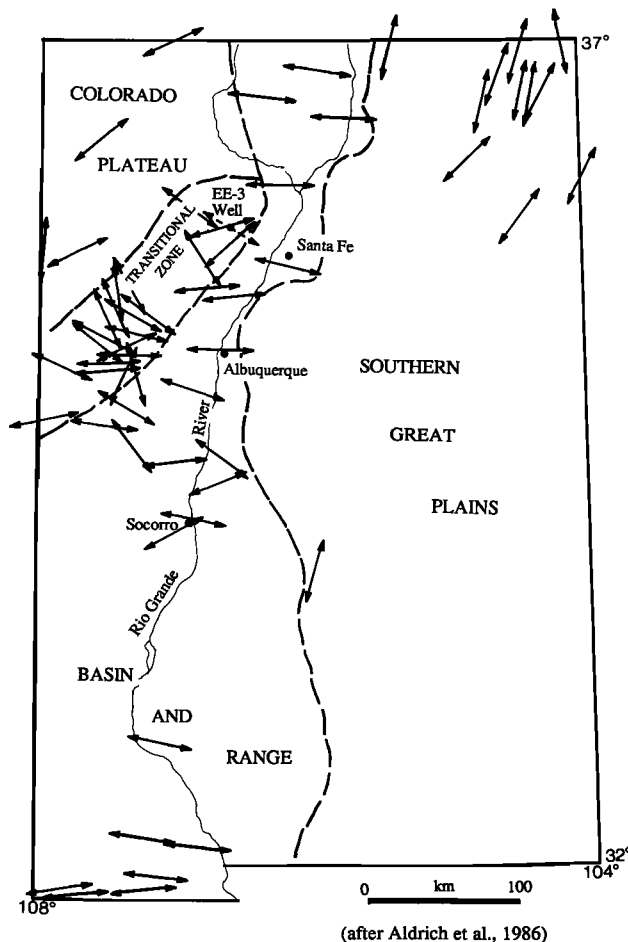


Fig. 1. Location map of the Fenton Geothermal well EE-3, stress trajectories indicate published values of the least horizontal principal stress (after Aldrich et al., 1986).

Copyright 1988 by the American Geophysical Union.

Paper number 7L7276.
0094-8276/88/007L-7276\$03.00

fluxgate magnetometer within the tool makes it possible to orient the data with respect to magnetic north.

Digital borehole televiewer data consists of the travel time and amplitude of each reflected pulse and were acquired through digitization of the analog recordings. The A/D processor utilizes programmable clocks triggered by the source pulse. The sampling rate used for digitization of this data was 1 μ sec, the A/D used has a 12 bit resolution with a data acquisition rate of 2.16 Mbits/s.

The televiewer logging in the Fenton EE-3 geothermal well was completed in January 1986 by the Denver U.S.G.S. Water Resources Division [A. Hess and R. Hodges, personal communication]. A standard 10.2 cm diameter, 1.4 MHz acoustic borehole televiewer was used to image the borehole wall over a 798 m depth interval. Two separate sections of this interval were logged; the lower from depth 3627 m to 3432 m and the upper interval from 2896 m to 2829 m producing a total of 262 meters of data. The log was run at a faster than normal rate of 10 cm/s producing an image with a scan line every 4 cm. The data are fair to poor quality, because the tool was off-center in the wellbore; temperatures in this well are approximately 325° C at 4.5 km depth resulting in an extremely difficult environment for televiewer operation.

The EE-3 well deviates by about 11° below depth 3150 m. Studies of the effects of borehole deviation on breakout azimuth indicate a dependence on fault regime [Mastin, 1988]. For a strike-slip fault stress state a borehole must deviate at least 35° from vertical to have a breakout azimuth differ more than 10° from S_{Hmin} . For a normal fault regime the critical angle is dependent upon the magnitudes of S_{Hmax} and S_{Hmin} , however, deviations less than about 10° do not affect breakout azimuths. The borehole deviation was therefore not considered to present a source of error in this analysis.

Data Analysis

A detailed analysis of the digital data was performed to measure borehole shape with depth. Figure 2a is a conceptual

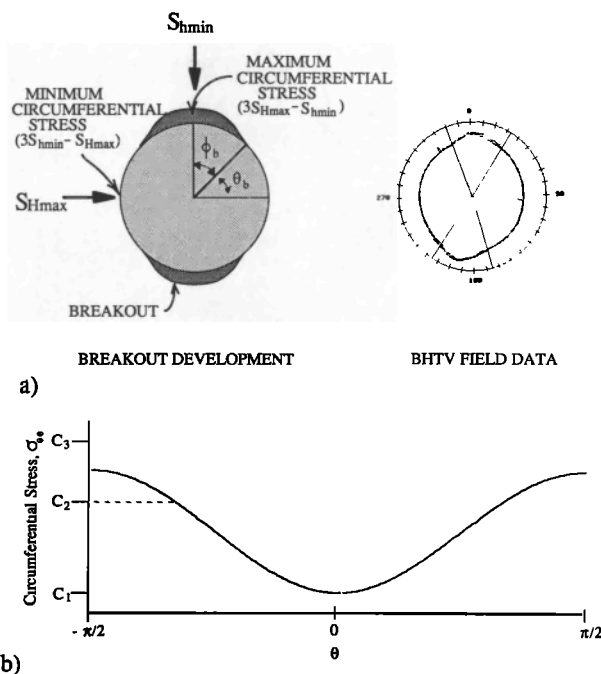


Fig. 2a) Schematic of the breakout process showing angle of breakout initiation ϕ_b , and BHTV data over a breakout interval where polar cross sections delineate the breakout shape. b) The variation in circumferential stress, σ_θ , with angle θ from S_{Hmax} .

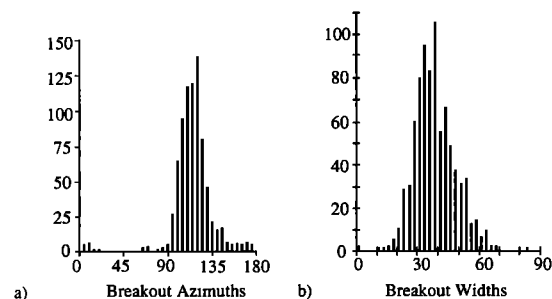


Fig. 3. Histograms of breakout azimuths (a) and widths (b) over a 262 meter interval in the Fenton well.

drawing of the development of a breakout [see theoretical shapes in Zoback, et al., 1985] along with a plot of field data which demonstrates the picking technique. The greater travel time within the breakout defines the characteristic breakout shape. Several superimposed scans of travel time data (representing a vertical distance of several cm in the well) are plotted in polar cross section to allow measurement of breakout azimuth and minimum breakout width. The data are corrected for tool position and magnetic declination before plotting. The objectives of this analysis are to obtain precise breakout azimuths and the minimum breakout width. Where there are continuous reflections from the broken out sections, as in the example in Figure 2a, the breakout width is easily determined. The two radial lines represent the picked angle of the breakout width and the breakout azimuth bisects this angle. Breakout azimuth should coincide with the direction of least horizontal principal stress. As discussed below, breakout width is important for estimation of stress magnitude.

Intervals of the EE-3 well 12 cm in length were evaluated through this interactive graphics routine. Where high quality data were recorded, it was possible to measure the azimuth and the width of breakout intervals. Over some intervals it was only possible to pick the breakout width on the northwest side of the borehole due to the missing data between azimuths 80° and 120°. These bands of missing data are the result of a non-centralized tool which causes non-normal incidence of the pulse at the borehole wall and subsequent deflection of the returned signal away from the transducer.

In the data analysis, the two sides of a breakout were picked independently; 928 separate breakout azimuths and 644 breakout widths were measured over a depth range of 262 m in the EE-3 well. The data were statistically reduced to obtain the mean direction of least principal horizontal stress after a method developed by Mardia [1972]. The mean direction is 119° and the standard deviation 9° (Figure 3a).

Thus, the orientation of least horizontal principal stress of N119°E in this study is similar to principal horizontal stress indicators of the Basin and Range and Rio Grande Rift and not aligned with stress indicators located in the Colorado Plateau (Figure 1, dashed trajectory). The orientation obtained in this study is significantly different from the N70°E orientation of least horizontal stress obtained from a shallow stress measurement made with hydrofracture methods at the Fenton site [see measurement #64, Aldrich and Laughlin, 1984].

Stress Magnitude Analysis

Failure of the borehole wall is due to the concentration of horizontal principal stresses. At the borehole wall, remote stresses are translated to radial and circumferential principal stress components in polar coordinates and become functions of r , the radius from the center of the borehole, and θ , the angle from maximum horizontal stress. Assuming one principal stress to be vertical and parallel to the borehole, the stress field at the borehole wall is completely described by normal stresses acting in the horizontal plane, σ_r and σ_θ and

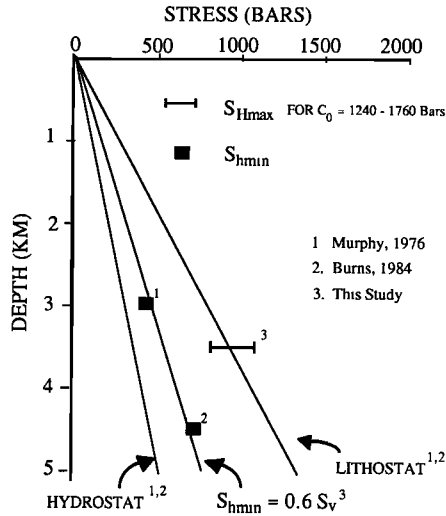


Fig. 4. Stress state for EE-3 well Fenton geothermal well. The pore pressure and vertical stress increase at a rate of 99 bars/km and 265 bars/km respectively. Theoretical S_{hmin} curve is 145 bars/km. Solid horizontal bar the range of S_{Hmax} calculated from breakout width for $C_0 = 1240$ to 1760 bars.

the vertical stress, σ_z . The presence of pore water affects the frictional behavior of rock; the effective normal stress is the actual normal stress less the pore pressure. The effective stress components in the vicinity of a circular hole are given by Kirsch [1898] and by Jaeger and Cook [1979]. At the borehole wall, the radial and shear effective stresses are zero and the stress field is defined by the circumferential and vertical stresses. The circumferential effective stress is:

$$\sigma_\theta = (\sigma_1 + \sigma_3) - 2(\sigma_1 - \sigma_3) \cos 2\theta - \Delta P_w \quad (1)$$

where σ_1 is the maximum and σ_3 the minimum effective horizontal principal stress, and ΔP_w is the absolute magnitude of the difference between the formation pore pressure and borehole fluid pressure. The value of ΔP_w for the EE-3 well is estimated to be about 13 bars based upon available drilling information.

Under conditions of unequal horizontal principal stresses and negligible ΔP_w , the circumferential stress has its maximum value at $\theta = \pi/2$ where $\sigma_\theta = 3S_{Hmax} - S_{hmin} - 2P_p$ and its minimum at $\theta = 0$ where $\sigma_\theta = 3S_{hmin} - S_{Hmax} - 2P_p$. Here S_{Hmax} and S_{hmin} are the principal horizontal stresses and P_p is the pore pressure.

The variation of circumferential stress as a function of azimuth is shown in Figure 2b for arbitrary values of S_{Hmax} and S_{hmin} . In this figure θ_b is the angle of breakout initiation with respect to S_{Hmax} and ϕ_b is the half width of the breakout ($\phi_b = \pi/2 - \theta_b$). Usually breakouts occur if the uniaxial compressive strength of the rock is exceeded by the concentrated circumferential stress. If the uniaxial compressive strength of the rock is sufficiently high, as at C3, the strength exceeds the concentrated circumferential stress and no breakouts occur. However, when the strength of the intact rock is exceeded by the concentrated stress, as at C2, the rock will fail in a restricted section of the borehole (see dashed line in Figure 2b). If the rock is sufficiently weak, as at C1, failure could occur at all azimuths.

In-situ principal stress differences in the crust can be constrained by assuming that the ratio of shear to normal stress on pre-existing faults does not exceed the frictional strength of the faults. In terms of principal stresses, the ratio of maximum to minimum effective principal stress is related to the coefficient of friction, μ , by:

$$\frac{\sigma_1}{\sigma_3} = \frac{S_1 - P_p}{S_3 - P_p} = (\sqrt{(\mu^2 + 1)} + \mu)^2 \quad (2)$$

[Jaeger and Cook, 1979]. Using Anderson's [1951] classification of faults the principal stresses are: $S_3 = S_{hmin}$ and $S_1 = S_v$ in a normal faulting environment; $S_3 = S_{hmin}$ and $S_1 = S_{Hmax}$ for strike-slip faulting; and $S_3 = S_v$ and $S_1 = S_{Hmax}$ for thrust faulting where S_v is the lithostatic load. Using reasonable values for μ of $0.6 < \mu < 1.0$ [Byerlee, 1978] bounds may be placed on the values of in-situ horizontal principal stresses in each faulting regime [see also Sibson, 1985; Brace and Kohlstedt, 1980; Zoback and Healy, 1984].

Seismicity studies at the Fenton site, which indicate extensional as well as strike-slip earthquake focal mechanisms, can be used to provide an independent estimate of S_{Hmax} [Fehler, et al., 1986; Dey, 1986]. The use of focal mechanisms to determine stress assumes a uniform stress field and that traction on the fault plane is parallel to the slip direction [A. Michael, 1987]. The coexistence of strike-slip and normal fault focal mechanisms implies that σ_1 and σ_2 interchange at the site and the difference between intermediate and maximum principal stress may be small [Wright, 1976; Angelier, 1979]. Assuming a value of $\mu = 0.6$ and hydrostatic pore pressure (which is appropriate for the EE-3 well) suggests that S_{hmin} is about $0.6 S_v$ (equation 2) and that S_{Hmax} is approximately equal to S_v . Figure 4 is the stress profile for the EE-3 well. Published estimates of S_{hmin} from hydraulic fracture experiments in this well and companion wells at the Fenton site (solid squares) are quite consistent with the theoretical value of $0.6 S_v$ [Murphy, 1976; Burns, 1984].

With knowledge of C_0 , S_{hmin} and breakout width the magnitude of maximum horizontal principal stress can be estimated by the breakout analysis. After the initial failure of the borehole wall upon breakout formation the circumferential stress decreases preventing widening of the breakouts. Thus, with time breakouts will deepen but do not widen [Zheng, written communication; Mastin, 1984; Zoback et al., 1985]. Aside from erosional effects on the initial shape of the breakout, such as fluid circulation or tool trips the angle ϕ_b should remain fairly constant (Figure 2). Using breakout geometry to determine stress magnitude was found to be limited by the time dependent failure processes that deepen the breakout [Zoback et al., 1986]. Utilizing only breakout width in this method avoids the problem of the time dependent growth of breakouts in depth.

At the borehole wall, the circumferential stress is given by equation 1 above. It may be assumed that at the maximum angle of breakout initiation, ϕ_b , the circumferential stress is just equal to the unconfined compressive rock strength, C_0 .

$$C_0 = \sigma_\theta = (\sigma_1 + \sigma_3) - 2(\sigma_1 - \sigma_3) \cos 2\theta - \Delta P_w \quad (3)$$

Converting from effective to principal stresses, using the effective stress law, $\sigma_{1eff} = \sigma_1 - \alpha P_p$ where α is assumed to be 1 for brittle failure of intact rock [Nur, 1971], we have:

$$S_{Hmax} = \frac{(C_0 + \Delta P_w + 2P_p)}{(1 - 2\cos 2\theta)} - S_{hmin} \frac{(1 + 2\cos 2\theta)}{(1 - 2\cos 2\theta)} \quad (4)$$

The width distribution of breakouts was determined over a 262 meter interval in the EE-3 well through the interactive graphics algorithm developed to analyze detailed borehole shape. Using all of the measured breakout widths the mean width over this interval is 38° (Figure 3b). Laboratory data from strength tests on core samples from the EE-3 well indicate a range of values for C_0 between 1240 and 1760 bars [T. Dey, personal communication]. The corresponding range of maximum horizontal principal stress magnitudes is 880 to 1080 bars (Figure 4, solid bar). The magnitude of S_{Hmax} in

this calculation has a nonlinear dependence on breakout width. Using the standard deviation in breakout width over the range of values for C_0 from 1240 to 1760 bars the error estimates are approximately ± 50 and ± 150 bars respectively.

Thus, the independently determined values for C_0 and SH_{min} , this analysis of breakout widths in the EE-3 well constrains the value of maximum horizontal principal stress to be approximately S_v , just as was predicted above from the occurrence of both strike-slip and extensional earthquakes in response to fluid injection at Fenton Hill. Thus, the calculated values of SH_{max} appear to be geologically reasonable for the Fenton site.

Conclusions

This detailed analysis of borehole shape using televue data recorded in the Fenton EE-3 well has provided a well resolved orientation of the horizontal principal stresses that agrees with other observation of the stress state at the Fenton site. The magnitude of the maximum horizontal compressive stress constrained by these data is consistent with the occurrence of both strike-slip and normal faulting focal mechanisms at this site. The analysis of breakout width may be a promising technique to estimate stress magnitude in drillholes where other techniques are not useful.

References

- Aldrich, M.J. and Laughlin, A.W., A model for the tectonic development of the Southeastern Colorado Plateau Boundary, *J. Geophys. Res.*, **89**, 10207 - 10218, 1984.
- Aldrich, M.J., Chapin, C.E. and Laughlin, A.W., Stress history and tectonic development of the Rio Grande rift, New Mexico, *J. Geophys. Res.*, **91**, 6199-6211, 1986.
- Anderson, E.M., *The dynamics of faulting and dyke formation with applications in Britain*, 2nd ed. Oliver and Boyd, Edinburgh, 1951.
- Angelier, J., Determination of the mean principal directions of stress for a given fault population: *Tectonophysics*, **56**, T17-26, 1979.
- Bell, J.S. and Gough D.I., Northeast-southwest compressive stress in Alberta: Evidence from oil wells. *Earth Planet. Sci. Lett.*, **45**, 475-482, 1979.
- Brace, W.F. and Kohlstedt, D.L., Limits on lithospheric stress imposed by laboratory experiments, *J. Geophys. Res.*, **85**, B11, 6248-6252, 1980.
- Burnes, K., Reconstruction of the stress field at Fenton Hill, in *Workshop on recent research in the Valles Caldera*, edited by G. Heiken, Los Alamos National Laboratory, Los Alamos, New Mexico, 1984.
- Byerlee, J.D., 1978. Friction of rocks. *Pure and Applied Geoph.*, **116**, 615-626.
- Chapin, C.E., and Cather, S.M., Eocene tectonics and sedimentation in the Colorado Plateau-Rocky Mountain area, in *Relations of the Tectonics to ore deposits in the Southern Cordillera*, edited by W. R. Dickenson and W. D. Payne, Ariz., Geol. Soc. Dig., **14**, 173-198, 1981.
- Cordell, L., Regional geophysical setting of the Rio Grande Rift, *Geol. Soc. Am. Bull.*, **89**, 1073-1090, 1978.
- Dey, T.N., State of stress in a hot dry rock reservoir at Fenton Hill, NM, *EOS*, **67**, 1206, 1986.
- Fehler, M., House, L., and Kaieda, H., Seismic monitoring of hydraulic fracturing, *27th U.S. Symposium on Rock Mechanics*, Univ. of Alabama, 606-613, 1986.
- Golombek, M.P., Geology, structure, and tectonics of the Pajarito fault zone in the Espanola basin of the Rio Grande Rift, New Mexico, *Geol. Soc. Am. Bul.*, **94**, 192 - 205, 1983.
- Gough, D.I. and Bell, J.S., Stress orientations from oil well fractures in Alberta and Texas, *Can. Journ. Earth Sci.*, **18**, 1358-1370, 1981.
- Hickman, S.H., Healy, J.H. and Zoback, M.D., In situ stress, natural fracture distribution, and borehole elongation in the Auburn geothermal well, Auburn, New York, *J. Geophys. Res.*, **90**, 5497-5512, 1985.
- Jaeger, J.C. and Cook, N.G.W., *Fundamental of rock mechanics*, 2nd ed., Methuen and Co., London, 1979.
- Kirsch, G., Die Theorie der Elastizitaet und die Beduerfnisse der Festigkeitslehre. *Zeitschrift VDI*, **29**, 797-807, 1898.
- Mardia, K.V., *Statistics of directional data*, Department of Mathematical Statistics, The University, Hull, England, Academic Press, London, 1972.
- Mastin, L., An analysis of stress-induced elongation of boreholes at depth, M.S. thesis, 241 pp., Stanford Univ, June, 1984.
- Mastin, L., The effect of borehole deviation on breakout orientation, *J. Geophys. Res.*, (in press), 1988.
- Michael, A.J., Use of focal mechanisms to determine stress: A control study. *J. Geophys. Res.*, **92**, 357-368, 1987.
- Murphy, H.D. Lawton, R.G., Tester, J.W., Potter, R.M., Brown, D.M. and Aamodt, R.L., Preliminary assessment of a geothermal energy reservoir formed by hydraulic fracturing. *Soc. of Pet. Eng 51 Annual Meeting*, New Orleans, 1976.
- Nur, A. and Byerlee, J., An exact effective stress law for elastic deformation of rock with fluids, *J. Geophys. Res.*, **76**, 6414-6419, 1971.
- Olsen, K.H., Braile, L.W., Stewart, J.N., Daudt, C.R., Keller, G.R., Ankeny, L.A. and Wolf, J.J., Jemez mountains volcanic field, New Mexico: Time term interpretation of the CARDEX seismic experiment and comparison with bouguer gravity, *J. Geophys. Res.*, **91**, 6175-6187, 1986.
- Plumb, R.A. and Cox, J.W., Deep crustal stress directions in North America from borehole elongation, *EOS*, **65**, 1984.
- Sibson, R.H., A note on fault reactivation, *J. Struct. Geology*, **7**, 6, 751-754, 1985.
- Wright, L., Late Cenozoic fault patterns and stress fields in the Great Basin and westward displacement of the Sierra Nevada block: *Geology*, **4**, 489-494, 1976.
- Zemanek, J., Glenn, E.E., Norton, L.J. and Caldwell, R.L., Formation evaluation by inspection with the borehole televue. *Geophysics*, **35**, 254-269, 1970.
- Zoback, M.D., Moos, D., Mastin, L., Anderson, R.N., Wellbore breakouts and in-situ stress, *J. Geophys. Res.*, **90**, 5523-5530, 1985.
- Zoback, M.D. and Healey, J.H., Friction, faulting, and in-situ stress. *Annales Geophysicae*, **2**, 689-698, 1984.
- Zoback, M.L. and Zoback, M.D., State of stress in the conterminous United States, *Journ. Geophys. Res.*, **85**, 6113-6156, 1980.
- Zoback, M.L. and Zoback, M.D., Tectonic stress field of the continental United States. In: *Geophysical framework of the Continental United States*, edited by L. Pakiser, and W. Mooney, GSA Memoir, 1988.
- C.A. Barton and M.D. Zoback, Stanford University, Department of Geophysics, Stanford, CA 94305.
- K.L. Burns, Los Alamos National Laboratory, ESS-1, MS-1981, Los Alamos, New Mexico 87045.

(Received: December 1, 1987;
revised: February 11, 1988;
accepted: February 11, 1988.)